



# Analysis of the Rotational Motion of a Solid Body in the Presence of External Moments

A. M. Farag<sup>1</sup>

Received: 1 October 2022 / Revised: 18 January 2023 / Accepted: 20 January 2023 / Published online: 7 February 2023  
© The Author(s) 2023

## Abstract

**Purpose** In this work, the vibrating motion of a dynamically symmetric solid body with an elastic string, around a fixed point, as a new model, is investigated.

**Hypotheses** The body spins as a result of external moments along the body's principal axes, such as perturbing, restoring, and gyrostatic moments. It has been supposed that this body has a rapid angular velocity at the beginning of motion in the direction of its symmetry dynamic axis.

**Methods** The averaging approach is employed to transform the governing system of motion into another appropriate averaging one to gain the asymptotic solutions of this system.

**Conclusion** These solutions are graphed and discussed in different plots depending on the numerical values of the body's physical properties. The positive effects of the gyrostatic moment vector on the motion are examined in some cases. Furthermore, the obtained results generalize the previously related studies.

**Applications** The importance of the investigated dynamical system is due to its applications in a variety of domains, including physics and engineering.

**Keywords** Symmetric solid body · Euler–Poisson equations · Averaging method · Gyrostatic and perturbing moments

## Introduction

Perturbation methods [1–3] had grasped the attention of many researchers throughout the past few decades to acquire the solutions for the rotatory motion of a rigid body (RB) problem [4–11]. It is reported that such a problem is regulated by six non-linear differential equations and three associated first integrals [12]. The solutions to these equations are only found in a few special cases [13], where the urgent fourth integral was discovered. There are several limitations in these circumstances regarding the location of the body's center of mass and the magnitudes of the main moments of inertia. To achieve this integral, a number of integrable scenarios have appeared, including [12, 14–18]. Six integrable scenarios for the RB were found in [14] when a body is being affected by an axisymmetric combination of gyroscopic and potential forces in accordance with initial circumstances. The author also looked at the

generalization of Lagrange's scenario, the Kovalevskaya case, and the body's full symmetric case. In [15], a transformation rotation with position-dependent angular velocity has been used to examine the generalization of the other six integrable situations. Two new criteria are used in [16] to provide the appropriate integrable situations for the rigid body motion similar to Kovalevskaya top. Additional requirements are constructed in [17], to generalize the integrable scenario of Chaplygin and Yehia. A brand-new class of 2D integrable systems with twenty arbitrary parameters is examined in [18]. The author provided an integrable situation of a third degree in velocities to generalize certain earlier cases. When the body rotates while being affected by a gyrostatic moment, the necessary and sufficient condition for getting the fourth first integral is stated in [12].

In [19], the authors investigated the behavior of a heavy ball rolling inside a semi-spherical chamber when subjected to horizontal kinematic excitation. This ball has been designed to make an excellent contact with the hollow surface without slipping at all. Harmonic horizontal excitation was taken into consideration during the numerical analysis of this problem. However, they examined the predictable and recognizable patterns of free motion of a tuned mass damper of the ball type in [20].

✉ A. M. Farag  
Afaf.hussien@science.tanta.edu.eg

<sup>1</sup> Mathematics Department, Faculty of Science, Tanta University, Tanta 31527, Egypt

The neighborhood of seven different limit solutions (or limit trajectories) has been discovered and physically explained. The movement of a big ball rolling inside a semi-spherical chamber in the presence of a kinematical excitation in a horizontal direction is simulated analytically and numerically in [21] and [22], respectively. In light of the Lagrangian governing system, an analytical approach is used to examine this movement.

There are many different approximations can be used to treat the difficulty in solving the nonlinear ordinary differential equations, such as the small parameter method (SPM), the Krylov–Bogoliubov–Mitropolski (KBM), and the averaging method (AM). The SPM is used in [4] and [5] to obtain the asymptotic solutions of the fast rotatory RB's motion when the uniform gravitational field and the Newtonian gravitational field are acted upon, respectively. On the other hand, these solutions contain singular points that are treated for ever in the works [6–8], when the authors thought about the action of the gyrostatic moment (GM) on the body, regardless of whether the gravitational field or the Newtonian one is applied. Furthermore, the approximate solutions of the 3D rotatory motion of a RB under the action of a Newtonian field, a magnetic one and the GM are examined in [9] using the SPM, in which the formulas of Euler's angles are derived. Recently, this method is utilized in [23] to examine the RB motion similar to the Bobylev–Steklov conditions when the body is forced by GM, electromagnetic field, and Newtonian field. Whereas in [24], the authors considered that the body's center of mass deviates somewhat from its dynamic axis of symmetry. The body is forced by one component of the GM and the electromagnetic field.

The approach of KBM was used in [10] to provide the approximate analytical solutions of the equations of motion (EOM) for a symmetrical case of the RB in a uniform gravity field. As before, these solutions include singular points. The generalization of this issue is found in [11] and [25] when a GM and a Newtonian field, respectively, have an effect on the body. The obtained results do not have any point of singularity at all, due to the use of Amer's frequency [6, 11, 25]. Recently, the RB problem is examined in [26] at the closeness of inertia's ellipsoid and rotation's ellipsoid. The authors considered the action of a uniform field only beside one component of the GM about the symmetry dynamic axis. The numerical solutions are obtained and compared with the analytical ones. Moreover, the treatment of this problem for the scenario of Euler and Poincaré is found recently in [27] using the KBM. In [28], the numerical outcomes of the EOM of a RB that is loaded with a rotating mass in the presence of a Newtonian field are discussed. The author considered that the body's center of mass is located in one of the planes of the moments of inertia.

On another level, the AM has met with the endorsement of numerous scientists to acquire the approximate solutions for the body's motion, whether under the influence of the gravitational field [29–37] or the Newtonian field [37–39]. In [30],

the authors studied the perturbed movement of the RB near a regular precession for Lagrange's scenario. A small parameter was introduced into the governing EOM in accordance with some initial circumstances. The rotatory problem of a dynamically spherical RB connected with a viscoelastic element was presented in [31]. This element has been represented by a moving mass that is coupled to the point on one of the main axes of inertia via a spring and damper. The motion is investigated in the context of a restoring moment, which is dependent on the nutation angle. Recently, the numerical solutions of this problem has been examined in [32] and [33], in light of the averaging system of the governing one, when the body is influenced by the moments of perturbing and restoring. In these works, it is considered that the body has a high starting angular velocity around the dynamic principal axis of inertia, in which it is subjected to the moments of perturbing at the principal axes directions. The AM is applied to gain the solutions of the EOM. Along with the previous moments, the rotational motion of this body is examined in [35] when the GM is acted in which its first components are considered to be zero. The extension of this work is included in [36] when the body is charged according to a subjected point charge on the dynamic symmetry axes and its position of mass is a bit displaced from this axis. In [37], the authors considered the action of the Newtonian field only, which is generalized in [38] and in [39] when the authors adopted the full activity of the GM and the action of the electromagnetic field, respectively. Some applications are concerned with the controlling of the angular velocity, linear dissipative moments, and the atmospheric case are considered in [34, 38, 39]. However, the numerical solutions of the symmetric body under the impact of the third projection of the GM and the Newtonian field are investigated in [40]. More contributions on the application of the AM procedure for various dynamical models can be found in [41].

This article deals with the rotational motion of a symmetric solid body around one fixed point with a fresh perspective, in which it rotates initially with a rapidly angular velocity around its dynamic symmetry axis. It is considered that the body rotates in the entity of GM and perturbing one around the inertia principal axes. The regulating system of the EOM is modulated to the averaging one applying the AM. The later system is solved analytically for some applications. The attained results are discussed and demonstrated in various plots for each application to show the effectiveness of several parameters on the body's behavior. These results generalize the previous works [29, 30], and [34].

## Description of the Problem

The major aim of the present section is to outline the rotational motion of a symmetric RB (having a mass  $m$ ) around one fixed point  $O$ . Let us consider two Cartesian orthogonal systems

having the same origin point  $O$ ; namely a fixed system  $OXYZ$  and a moving one  $Oxyz$  which is immovable in the body but moving with it, and it is directed on the body's inertia principal axes. The body is supposed to be connected from its upper point  $N_1$  with a spring (of stiffness  $\nu$ ), in which its second end  $N_2$  is positioned on the axis  $OZ$  at a distance  $d$  from  $O$ . Therefore, we consider  $N_1N_2 = S(\theta)$ ,  $\theta \neq 0$ , where  $\theta$  is the angle between  $Oz$  and  $OZ$ . The investigated motion is considered under the disposal of a perturbing moment vector  $\underline{M}$  and a gyrostatic one  $\underline{\ell}$ ; in which their projections  $M_j$  and  $\ell_j$  ( $j = 1, 2, 3$ ) are acted about the body's principal axes  $Ox$ ,  $Oy$ , and  $Oz$  (Fig. 1).

The governing system of EOM can be acquired using the next angular momentum equation [38]

$$\dot{\underline{h}}_O + \underline{\omega} \wedge \underline{h}_O = \underline{L}_O,$$

where

$$\underline{h}_O \equiv (I_1 p + \ell_1, I_2 q + \ell_2, I_3 r + \ell_3),$$

$$\underline{L}_O = mg(\underline{\gamma} \wedge \underline{Oc}) + \underline{M}.$$

Here,  $\underline{h}_O$  and  $\underline{L}_O$  are the vectors of angular momentum and the moment of all applied forces at  $O$ , respectively. The dots refer to the time's differentiation,  $\underline{\omega} \equiv (p, q, r)$  is the vector of angular velocity,  $\underline{Oc} = \underline{l} \equiv (0, 0, l)$  represents the position

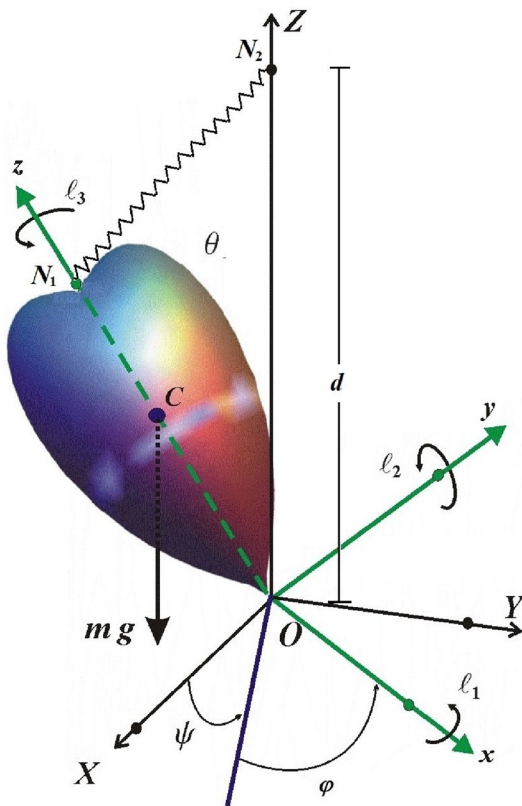


Fig. 1 The dynamical model

vector of the center of mass,  $g$  is the gravitational acceleration,  $I_j$  ( $j = 1, 2, 3$ ) are the inertia's principal moments, and  $\underline{\gamma} \equiv (\sin \theta \sin \varphi, \sin \theta \cos \varphi, \cos \theta)$  is the unit in the direction of  $Z$ -axis, in which  $\varphi$  is the angle of self-rotation.

It is worthy to mention that the angular velocity projections  $p, q$ , and  $r$  can be written in terms of the Euler's angles  $\theta, \varphi$ , and  $\psi$  in the following forms [13]

$$p = \dot{\psi} \sin \varphi \sin \theta + \dot{\theta} \cos \varphi,$$

$$q = \dot{\psi} \cos \varphi \sin \theta - \dot{\theta} \sin \varphi,$$

$$r = \dot{\varphi} + \dot{\psi} \cos \theta,$$

in which  $\theta$  and  $\psi$  are the nutation and precession angles, respectively.

Based on the above simulation, we can conclude that the acting forces of the body are the gravity force and the spring elastic's force  $F$ , in which its modulus is directly regulated with the spring's deformation, i.e.,  $F = \nu(S - S_0)$  where  $S_0 = N_1N_2$  at  $\theta = 0$  is the un-deformed length of the spring. Therefore, along the body's main axis, the restoring torque is composed as follows

$$\underline{M}_{\text{restoring}} = (u \sin \theta \cos \varphi, -u \sin \theta \sin \varphi, 0);$$

$$u = mg l + \nu d z^* [1 - S_0(d^2 + z^{*2} - 2dz^* \cos \theta)^{-1/2}], \quad (1)$$

$$z^* = ON_1, \quad d = ON_2.$$

After grasping the previous, the EOM with respect to the Cartesian system  $Oxyz$  can be expressed in the form

$$I_1 \dot{p} + (I_3 - I_1) qr + q \ell_3 - r \ell_2 = u \cos \varphi \sin \theta + M_1,$$

$$I_1 \dot{q} + (I_1 - I_3) rp - p \ell_3 + r \ell_1 = -u \sin \varphi \sin \theta + M_2,$$

$$I_3 \dot{r} + p \ell_2 - q \ell_1 = M_3,$$

$$\dot{\theta} = -q \sin \varphi + p \cos \varphi, \quad (2)$$

$$\dot{\varphi} = r - (q \cos \varphi + p \sin \varphi) \cot \theta,$$

$$\dot{\psi} = (q \cos \varphi + p \sin \varphi) \csc \theta.$$

Here, it is considered that  $I_1 = I_2$  for the studied symmetric case. According to the above EOM, one can obtain the governing EOM of Lagrange's case at  $\underline{\ell} \equiv \underline{0}$ ,  $\underline{M} \equiv \underline{0}$ , and  $u = \text{const}$ . Moreover, the governing system in [29, 30], and [34] can be obtained at  $\underline{\ell} \equiv \underline{0}$ , in which the same approach of these works is used in the analysis of the present work.

It is supposed that at the start of motion, the body spins around the dynamic symmetry axis with rapid angular velocity, the first two components of  $\underline{M}$  are less than  $u$  while its third component is approximately order of  $u$ . Therefore, one can write

$$p^2 + q^2 \ll r^2, I_3 r^2 \gg u, |M_i| \ll u, M_3 \approx u (i = 1, 2). \quad (3)$$

Now, we are going to introduce a small parameter  $\varepsilon$  to apply the AM. Therefore, the previous conditions (3) can be interpreted as follows

$$\begin{aligned}
 p &= \varepsilon P, q = \varepsilon Q, u = \varepsilon U, \quad \ell_i = \varepsilon \ell_i^* \\
 M_i &= \varepsilon^2 M_i^*(P, Q, r, \psi, \theta, \varphi, \tau); \quad (i = 1, 2), \\
 M_3 &= \varepsilon M_3^*(P, Q, r, \psi, \theta, \varphi, \tau), \quad \tau = \varepsilon t.
 \end{aligned}
 \tag{4}$$

Here, the variables  $Q, P$ , and the functions  $M_i^*, U$  are considered to be limited values of unity at  $\varepsilon \rightarrow 0$  such as  $r, \psi, \theta$ , and  $I_1, I_3$ .

It is remembered that the goal of the present work is to achieve the solutions of the EOM (2) in the presence of conditions (3) and equalities (4) using the AM [1, 2].

### The Averaging Method (AM)

Our aim in this part is to get the averaging system of the corresponding controlling one of the EOM (2). Therefore, the AM is used to achieve the desired system. To acquire this aim, making use of (4) into (2), and then cancelling  $\varepsilon$  from both sides of the resulted system to yield

$$\begin{aligned}
 I_1 \dot{P} + (I_3 - I_1) Qr + Q \ell_3 - r \ell_2^* &= U \sin \theta \cos \varphi + \varepsilon M_1^*, \\
 I_1 \dot{Q} + (I_1 - I_3) rP + r \ell_1^* - P \ell_3 &= -U \sin \theta \sin \varphi + \varepsilon M_2^*, \\
 I_3 \dot{r} &= \varepsilon \ell_1 Q - \varepsilon \ell_2 P + \varepsilon M_3^*, \\
 \dot{\theta} &= \varepsilon (-Q \sin \varphi + P \cos \varphi), \\
 \dot{\varphi} &= r - \varepsilon (Q \cos \varphi + P \sin \varphi) \cot \theta, \\
 \dot{\psi} &= \varepsilon (Q \cos \varphi + P \sin \varphi) \csc \theta.
 \end{aligned}
 \tag{5}$$

To achieve the desired solutions, we begin with the approximation at  $\varepsilon = 0$ . Consequently, the solutions of the final four equations in the aforementioned system are

$$r = r_0, \quad \theta = \theta_0, \quad \varphi = r_0 t + \varphi_0, \quad \psi = \psi_0, \quad U_0 = U(\theta_0),
 \tag{6}$$

where  $r_0, \theta_0, \varphi_0$ , and  $\psi_0$  are the constants of integration that correspond to the variables at the beginning of the motion.

Inserting (6) into the first two equations of (5) when  $\varepsilon = 0$ , and then the derivatives of the resulted two equations produce

$$\begin{aligned}
 \dot{P} + y_0^2 P &= U_0 Z_0 \sin \theta_0 \sin(r_0 t + \varphi_0) + y_0 r_0 I_1^{-1} \ell_1^*, \\
 \dot{Q} + y_0^2 Q &= U_0 Z_0 \sin \theta_0 \cos(r_0 t + \varphi_0) + y_0 r_0 I_1^{-1} \ell_2^*.
 \end{aligned}
 \tag{7}$$

The nonlinear system described above has two degrees of freedom, and its integration yields

$$\begin{aligned}
 P &= a \cos \gamma_0 + b \sin \gamma_0 + E_0 \sin \theta_0 \sin(r_0 t + \varphi_0) + (I_1 y_0)^{-1} r_0 \ell_1^*, \\
 Q &= a \sin \gamma_0 - b \cos \gamma_0 + E_0 \sin \theta_0 \cos(r_0 t + \varphi_0) + (I_1 y_0)^{-1} r_0 \ell_2^*,
 \end{aligned}
 \tag{8}$$

where

$$\begin{aligned}
 a &= P_0 - E_0 \sin \theta_0 \sin \varphi_0 - (I_1 y_0)^{-1} r_0 \ell_1^*, \\
 b &= -Q_0 + E_0 \sin \theta_0 \cos \varphi_0 + (I_1 y_0)^{-1} r_0 \ell_2^*, \\
 \gamma_0 &= y_0 t, \quad n_0 = (I_3 - I_1) r_0 I_1^{-1}, \\
 E_0 &= U_0 / [I_1(y_0 + r_0)], \quad |y_0 / r_0| \leq 1, \quad r_0 \neq 0, \\
 y_0 &= n_0 + I_1^{-1} \ell_3, \quad Z_0 = (y_0 - r_0) I_1^{-1}.
 \end{aligned}$$

Here  $P_0 = P_{t=0}, Q_0 = Q_{t=0}, \gamma_0$  refer to the generating system oscillation phase, and  $a, b$  represent the van der Pol type of the osculating variables [30].

Since Eq. (5) constitute a nonlinear system, we can insert  $\gamma = \gamma(t)$  as a new variable, to transform this system to an autonomous one, according to

$$\dot{\gamma} = y, \quad \gamma(0) = 0; \quad y = I_1^{-1} [(I_3 - I_1) r + \ell_3].
 \tag{9}$$

Based on (6) and (8) at  $\varepsilon = 0$ , the general solutions of (5) can be estimated. The variables  $Q$  and  $P$  can be expressed in an alternative form as follows

$$\begin{aligned}
 P &= a \cos \gamma + b \sin \gamma + E \sin \theta \sin \varphi + (I_1 y)^{-1} r \ell_1^*, \\
 Q &= a \sin \gamma - b \cos \gamma + E \sin \theta \cos \varphi + (I_1 y)^{-1} r \ell_2^*.
 \end{aligned}
 \tag{10}$$

Therefore, in accordance with (10),  $a$  and  $b$  can be written as the next form

$$\begin{aligned}
 a &= Q \sin \gamma + P \cos \gamma \\
 &\quad - E \sin \theta \sin \alpha - (I_1 y)^{-1} r (\ell_1^* \cos \gamma + \ell_2^* \sin \gamma), \\
 b &= -Q \cos \gamma + P \sin \gamma \\
 &\quad + E \sin \theta \cos \alpha - (I_1 y)^{-1} r (\ell_1^* \sin \gamma - \ell_2^* \cos \gamma); \\
 \alpha &= \gamma + \varphi.
 \end{aligned}
 \tag{11}$$

Let us reconsider the system of Eq. (5) at  $\varepsilon \neq 0$  beside Eq. (10) and according to the above discussion, we can alter  $P, Q, r, \psi, \theta, \varphi$ , and  $\gamma$  in (5) and (9) to obtain the  $a, b, r, \psi, \theta, \alpha$ , and  $\gamma$  as new variables. From (11), the following form can be obtained through various manipulations and reductions

$$\begin{aligned}
 \dot{a} &= \varepsilon I_1^{-1} (M_1^0 \cos \gamma + M_2^0 \sin \gamma) \\
 &\quad - \varepsilon (I_1 y)^{-2} I_3^{-1} M_3^0 \ell_3 (\ell_1^* \cos \gamma + \ell_2^* \sin \gamma) \\
 &\quad - \varepsilon E \cos \theta [b - E \sin \theta \cos \alpha + (I_1 y)^{-1} \\
 &\quad r (\ell_1^* \sin \gamma - \ell_2^* \cos \gamma)] + I_1^{-1} \sin \theta \times \cos \alpha \\
 &\quad [U - E (I_3 r + \ell_3)] - \varepsilon U [I_1(y + r)]^{-2} M_3^0 \\
 &\quad \sin \theta \sin \alpha + \varepsilon v d^2 z^* s_0 [I_1(y + r)]^{-1} \sin^2 \theta \\
 &\quad (d^2 + z^*{}^2 - 2dz^* \cos \theta)^{-3/2} [a \cos \alpha \sin \alpha \\
 &\quad + b \sin^2 \alpha + (I_1 y)^{-1} r \sin \alpha (\ell_1^* \cos \varphi - \ell_2^* \sin \varphi)],
 \end{aligned}$$

$$\begin{aligned} \dot{b} = & \varepsilon I_1^{-1}(M_1^0 \sin \gamma - M_2^0 \cos \gamma) \\ & - \varepsilon (I_1 y)^{-2} I_3^{-1} M_3^0 \ell_3 (\ell_1^* \sin \gamma - \ell_2^* \cos \gamma) \\ & + \varepsilon E \cos \theta [a + E \sin \theta \sin \alpha + (I_1 y)^{-1} r \\ & (\ell_1^* \cos \gamma + \ell_2^* \sin \gamma)] + I_1^{-1} \sin \theta \sin \alpha \\ & \times [U - E(I_3 r + \ell_3)] - \varepsilon [I_1(y+r)]^{-2} U M_3^0 \\ & \sin \theta \cos \alpha + \varepsilon v d^2 z^{*2} s_0 [I_1(y+r)]^{-1} \sin^2 \theta \\ & (d^2 + z^{*2} - 2dz^* \cos \theta)^{-3/2} [a \cos^2 \alpha + b \\ & \sin \alpha \cos \alpha + (I_1 y)^{-1} r \cos \alpha (\ell_1^* \cos \varphi - \ell_2^* \sin \varphi)], \end{aligned} \tag{12}$$

$$\begin{aligned} \dot{r} = & \varepsilon I_3^{-1} [M_3^0 + \varepsilon I_3(Q \ell_1^* - P \ell_2^*)], \\ \dot{\theta} = & \varepsilon [a \cos \alpha + b \sin \alpha + (I_1 y)^{-1} r (\ell_1^* \cos \varphi - \ell_2^* \sin \varphi)], \\ \dot{\psi} = & \varepsilon [a \sin \alpha - b \cos \alpha + E \sin \theta \\ & + (I_1 y)^{-1} r (\ell_1^* \sin \varphi + \ell_2^* \cos \varphi)] \csc \theta, \\ \dot{\alpha} = & I_1^{-1} (I_3 r + \ell_3) - \varepsilon [a \sin \alpha - b \cos \alpha + E \sin \theta \\ & + (I_1 y)^{-1} r (\ell_1^* \sin \varphi + \ell_2^* \cos \varphi)] \cot \theta, \\ \dot{\gamma} = & I_1^{-1} [(I_3 - I_1) r + \ell_3], \end{aligned}$$

where

$$M_j^0(a, b, r, \psi, \theta, \alpha, \gamma, \tau) = M_j^*(P, Q, r, \psi, \theta, \varphi, \tau), \quad j = 1, 2, 3.$$

A closer look at the above system (12) reveals that this system has slow variables  $a, b, r, \psi, \theta, \tau$ , and the fast ones  $\alpha, \gamma$ . It is obvious that system (12) is considered to be more general than the systems considered in [29, 30], and [34] at  $\ell_j = 0, \underline{M} \neq \underline{M}(\tau)$  ( $j = 1, 2, 3$ ).

Taking into consideration that  $M_j = M_j(t)$  and therefore it is very difficult to apply the AM which is due to that system (12) is nonlinear. Then, we consider a simple case of dependence on the variable  $\tau$ . According to the periodicity of  $M_j$  with the period  $2\pi$  in  $\varphi$ , then referring to (8) we find that  $M_j^{(0)}$  are also periodic function with period  $2\pi$  in  $\alpha$  and  $\gamma$ . It is clear that the frequencies  $\omega_\alpha = I_1^{-1}(I_3 r + \ell_3)$  and  $\omega_\gamma = I_1^{-1}[(I_3 - I_1) r + \ell_3]$  of system (12) correspond the phases  $\alpha$  and  $\gamma$ . The axial projection  $r$  of  $\underline{\omega}$  and the component  $\ell_3$  of the GM represent the backbone of these frequencies. Consequently, two pending cases can be examined when system (12) is averaged. The first case is the non-resonance which is occurring when  $\omega_\alpha$  and  $\omega_\gamma$  are non-commensurable i.e.,  $(I_3 r + \ell_3)/I_1 r \neq \hbar/\mathfrak{S}$  is an irrational number. The second one is the resonance which occurs for the commensurable frequencies i.e.,  $(I_3 r + \ell_3)/I_1 r = \hbar/\mathfrak{S} < 2; \hbar, \mathfrak{S}$  are prime natural numbers.

According to the first case  $(I_3 r + \ell_3)/I_1 r \neq \hbar/\mathfrak{S}$ , one obtains the approximate averaging system up to the first approximation by the way of averaging the right sides of

(12) relative to  $\alpha$  and  $\gamma$ . Considering  $\tau = \varepsilon t$  and omitting  $\varepsilon$  from the sides of (12) we get

$$\begin{aligned} a' = & I_1^{-1} \mu_1 - b U (I_3 r + \ell_3)^{-1} \cos \theta + U [(I_3 r + \ell_3)^{-2} \sin \theta \mu_3^s \\ & - [(I_3 - I_1) r + \ell_3]^{-2} I_3^{-1} \ell_3 \mu_4 + \frac{b}{2} (I_3 r + \ell_3)^{-1} \sin^2 \theta v d^2 z^{*2} s_0 \\ & \times (d^2 + z^{*2} - 2dz^* \cos \theta)^{-3/2}, \\ b' = & I_1^{-1} \mu_2 + a U (I_3 r + \ell_3)^{-1} \cos \theta - U (I_3 r + \ell_3)^{-2} \sin \theta \mu_3^c \\ & - [(I_3 - I_1) r + \ell_3]^{-2} I_3^{-1} \ell_3 \mu_5 + \frac{a}{2} (I_3 r + \ell_3)^{-1} \sin^2 \theta v d^2 z^{*2} s_0 \\ & \times (d^2 + z^{*2} - 2dz^* \cos \theta)^{-3/2}, \\ r' = & I_3^{-1} \mu_3, \quad \theta' = 0, \quad \psi' = U (I_3 r + \ell_3)^{-1}, \\ \gamma' = & I_1^{-1} [\ell_3 + (I_3 - I_1) r], \\ a' = & I_1^{-1} (\ell_3 + I_3 r) - U (\ell_3 + I_3 r)^{-1} \cos \theta. \end{aligned} \tag{13}$$

The primes here, denote the differentiation with respect to  $\tau$  and

$$\begin{aligned} \mu_1 = & \frac{1}{4\pi^2} \int_0^{2\pi} \int_0^{2\pi} (M_1^0 \cos \gamma + M_2^0 \sin \gamma) d\alpha d\gamma, \\ \mu_2 = & \frac{1}{4\pi^2} \int_0^{2\pi} \int_0^{2\pi} (M_1^0 \sin \gamma - M_2^0 \cos \gamma) d\alpha d\gamma, \\ \mu_3 = & \frac{1}{4\pi^2} \int_0^{2\pi} \int_0^{2\pi} M_3^0 d\alpha d\gamma, \\ \mu_3^s = & \frac{1}{4\pi^2} \int_0^{2\pi} \int_0^{2\pi} M_3^0 \sin \alpha d\alpha d\gamma, \\ \mu_3^c = & \frac{1}{4\pi^2} \int_0^{2\pi} \int_0^{2\pi} M_3^0 \cos \alpha d\alpha d\gamma, \\ \mu_4 = & \frac{1}{4\pi^2} \int_0^{2\pi} \int_0^{2\pi} M_3^0 (\ell_1^* \cos \gamma + \ell_2^* \sin \gamma) d\alpha d\gamma, \\ \mu_5 = & \frac{1}{4\pi^2} \int_0^{2\pi} \int_0^{2\pi} M_3^0 (\ell_1^* \sin \gamma - \ell_2^* \cos \gamma) d\alpha d\gamma. \end{aligned}$$

It is important to note that the moment  $U$  and its derivatives depend on  $\tau$ . Therefore, some applications will be discussed in the next section for the gyrostatic perturbed motion.

### Applications

The main goal of this part of the paper is to study some applications and to extend the results of the works [29, 30], and [34] for the considered gyrostatic motion utilizing the AM.

### The Case of Linear Dissipative Moment

Here, we are going to express  $M_j(j = 1, 2, 3)$  in terms of the slow time parameter  $\tau$  according to the next forms

$$\begin{aligned} M_1 &= -\varepsilon^2 (A_1 \sin^2 \tau) P, \\ M_2 &= -\varepsilon^2 (A_1 \sin^2 \tau) Q, \\ M_3 &= -\varepsilon (A_3 \cos^2 \tau) r, \end{aligned} \tag{14}$$

where  $A_1$  and  $A_3$  are constants, in which they are depending on the properties of the body. These projections are given in terms of the small parameter  $\varepsilon$ , in which their influence is focused in the direction of the third principal axis  $Oz$ , while the other two components have lower values along the axes  $Ox$  and  $Oy$ .

Making use of (14) into (13), and then applying some mathematical reduction to get the approximate solutions of (13) as

$$\begin{aligned} a(\tau) &= \exp\left[\frac{-A_1}{2I_1}\left(\tau - \frac{1}{2}\sin 2\tau\right)\right] [P_0 \cos \beta + Q_0 \sin \beta \\ &\quad - U_0 (I_3 r_0 + \ell_3)^{-1} \sin \theta_0 \sin(\beta + \varphi_0)], \\ b(\tau) &= \exp\left[\frac{-A_1}{2I_1}\left(\tau - \frac{1}{2}\sin 2\tau\right)\right] [P_0 \sin \beta - Q_0 \cos \beta \\ &\quad + U_0 (I_3 r_0 + \ell_3)^{-1} \sin \theta_0 \cos(\beta + \varphi_0)], \\ r(\tau) &= r_0 \exp\left[\frac{-A_3}{2I_3}\left(\tau + \frac{1}{2}\sin 2\tau\right)\right], \quad \theta = \theta_0, \\ \psi &= \psi_0 + Ud^*, \\ \beta &= [U \cos \theta_0 + \frac{1}{2} \sin^2 \theta_0 \nu d^2 z^{*2} s_0 (d^2 + z^{*2} - 2dz^* \cos \theta_0)^{-3/2}] d^*, \\ d^* &= \frac{1}{\ell_3} \sum_{n=0}^{\infty} \sum_{m=0}^{\infty} (-1)^{n+m} \left(\frac{I_3 r_0}{\ell_3}\right)^n \left(\frac{nA_3}{2I_3}\right)^m \int_0^\tau \left(k + \frac{1}{2} \sin 2k\right)^m dk. \end{aligned} \tag{15}$$

Referring to this system, we conclude that the behavior of the angle  $\theta$  has a stationary manner in which it equals the initial value. The axial velocity  $r$  has a decreasing exponentially behavior, i.e. it has a stable manner. A closer look to the expressions of  $a$  and  $b$  reveals that these expressions are dependently on the values of  $A_1$ . Therefore, the values of  $A_1$  and  $\tau$  effect on their manners, in which they are exponentially vanishing according to these values. According to the value of the convergence term  $d^*$ , the precession angle  $\psi$  has an increasing manner.

Substituting from (15) about  $a$ ,  $b$ , and  $r$  into (10) and (4), one can get

$$\begin{aligned} p &= \exp\left[\frac{-A_1}{2I_1}\left(\tau - \frac{1}{2}\sin 2\tau\right)\right] \\ &\quad \{-q_0 \sin(\gamma - \beta) + p_0 \cos(\gamma - \beta) + u_0 (I_3 r_0 + \ell_3)^{-1} \sin(\gamma - \beta - \varphi_0) \sin \theta_0\} \\ &\quad + u \{\sin \varphi \sin \theta_0 \{I_3 r_0 \exp\left[\frac{-A_3}{2I_3}\left(\tau + \frac{1}{2}\sin 2\tau\right)\right] + \ell_3\}^{-1}\} \\ &\quad + \left\{I_3 - I_1 + \ell_3 r_0^{-1} \exp\left[\frac{A_3}{2I_3}\left(\tau + \frac{1}{2}\sin 2\tau\right)\right]\right\}^{-1} \\ \ell_1, q &= \exp\left[\frac{-A_1}{2I_1}\left(\tau - \frac{1}{2}\sin 2\tau\right)\right] [q_0 \cos(\gamma - \beta) \\ &\quad + p_0 \sin(\gamma - \beta) - u_0 (I_3 r_0 + \ell_3)^{-1} \cos(\gamma - \beta - \varphi_0) \sin \theta_0] \\ &\quad + u \{\cos \varphi \sin \theta_0 \{I_3 r_0 \exp\left[\frac{-A_3}{2I_3}\left(\tau + \frac{1}{2}\sin 2\tau\right)\right] + \ell_3\}^{-1}\} \\ &\quad + \{I_3 - I_1 + \ell_3 r_0^{-1} \exp\left[\frac{A_3}{2I_3}\left(\tau + \frac{1}{2}\sin 2\tau\right)\right]\}^{-1} \ell_2, \\ \gamma &= I_1^{-1} \left\{ \ell_3 \tau + (I_3 - I_1) r_0 \left[ \int_0^\tau \sum_{m=0}^{\infty} (-1)^m \left(\frac{A_3}{2I_3}\right)^m \left(k + \frac{1}{2} \sin 2k\right)^m dk \right] \right\}. \end{aligned} \tag{16}$$

Here, one concludes that the first two projections  $p$  and  $q$  of  $\underline{\omega}$  are expressed in terms of  $p_0, q_0, \theta_0$ , and  $u_0$ , in which their behaviors have an exponentially decreasing which elucidates that they have stable manners. It is noted that  $(\ell_1, \ell_3)$  and  $(\ell_2, \ell_3)$  have a good significance on the behavior of  $p$  and  $q$ , respectively. Finally, it is obvious that  $\gamma$  has an increasing behavior with time.

The difference between the obtained results and the previous ones in [29, 30], and [34] can be represented by all terms that depend on components of the GM  $\ell_j (j = 1, 2, 3)$ . As a result, the results of this work can be used to obtain some limited cases, such as in the previously mentioned works at  $\ell_j = 0$ .

### Controlling the Projections of $\underline{\omega}$

This subsection investigates the case of regular precession of the studied problem. As a result, we can consider the moments under the following small control constraints in the forms

$$\begin{aligned} M_1 &= \frac{-\varepsilon^2 p^*}{(1 + \tau^2)(p^{*2} + q^{*2})^{1/2}}, \quad M_2 = \frac{-\varepsilon^2 q^*}{(1 + \tau^2)(p^{*2} + q^{*2})^{1/2}}, \\ M_3 &= \varepsilon e^{-\tau}, \\ p^* &= P - U(I_3 r + \ell_3)^{-1} \sin \theta \sin \varphi - [(I_3 - I_1) r + \ell_3]^{-1} r \ell_1^*, \\ q^* &= Q - U(I_3 r + \ell_3)^{-1} \sin \theta \cos \varphi - [(I_3 - I_1) r + \ell_3]^{-1} r \ell_2^*, \end{aligned} \tag{17}$$

The above Eq. (17) describes the suppression of time-optimal for the components  $p^*$  and  $q^*$  of the angular velocity [42] associated with the regular precession. Referring to (4), (10), and (17) we can write

$$\begin{aligned}
 M_1 &= -\varepsilon^2 \frac{a \cos \gamma + b \sin \gamma}{(1 + \tau^2)(a^2 + b^2)^{1/2}}, \\
 M_2 &= -\varepsilon^2 \frac{a \sin \gamma - b \cos \gamma}{(1 + \tau^2)(a^2 + b^2)^{1/2}}, \\
 M_3 &= \varepsilon e^{-\tau}.
 \end{aligned}
 \tag{18}$$

Substituting (18) into (13) and integrating the resulting equations to obtain

$$\begin{aligned}
 a(\tau) &= R_1(\tau) [P_0 \cos \chi + Q_0 \sin \chi - U_0 (I_3 r_0 + \ell_3)^{-1} \sin \theta_0 \sin(\chi + \varphi_0)], \\
 b(\tau) &= R_1(\tau) [P_0 \sin \chi - Q_0 \cos \chi + U_0 (I_3 r_0 + \ell_3)^{-1} \sin \theta_0 \cos(\chi + \varphi_0)], \\
 r(\tau) &= r_0 + I_3^{-1} (1 - e^{-\tau}), \quad \theta = \theta_0, \quad \psi = \psi_0 + U R_2(\tau), \\
 \chi &= \left[ U \cos \theta_0 + \frac{1}{2} \sin^2 \theta \sqrt{d^2 z^{*2} s_0 (d^2 + z^{*2} - 2d z^* \cos \theta)^{-3/2}} \right] R_2(\tau), \\
 R_1(\tau) &= \left[ 1 - \frac{I_1^{-1} \tan^{-1} \tau}{(a_0^2 + b_0^2)^{1/2}} \right], \quad R_2(\tau) = (1 + I_3 r_0 + \ell_3)^{-1} \left[ \tau + \sum_{n=1}^{\infty} \left( \frac{1 - e^{-n\tau}}{(1 + I_3 r_0 + \ell_3)^n} \right) \right].
 \end{aligned}
 \tag{19}$$

It is obvious that the angle  $\theta$  of nutation has a stationary value that equals its initial value. The projection  $r$  of  $\underline{\omega}$  exhibits an increasing behavior due to the excellent effect of the value of  $r_0$ , in addition to the value of  $I_3$  and the slow time parameter  $\tau$ . As described in the above case, the variables  $a$  and  $b$  depend upon the constants  $p_0, q_0, \theta_0, u_0$  besides the component  $\ell_3$  of the moment  $\underline{\ell}$ . Moreover, the time history of the precession angle  $\psi$  has an increasing monotonic behavior.

Utilizing (19), (10), and (4), one obtains the formulas of  $p, q$ , and  $\gamma$  as follows

$$\begin{aligned}
 p &= R_1(\tau) [-q_0 \sin(\gamma - \chi) + p_0 \cos(\gamma - \chi) \\
 &\quad + u_0 (I_3 r_0 + \ell_3)^{-1} \times \sin \theta_0 \sin(\gamma - \chi - \varphi_0)] \\
 &\quad + u (1 + I_3 r_0 + \ell_3 - e^{-\tau})^{-1} \sin \theta_0 \sin \varphi \\
 &\quad + (I_3 - I_1)^{-1} \{ 1 + \ell_3 (I_3 - I_1) [r_0 + I_3^{-1} (1 - e^{-\tau})]^{-1} \} \ell_1, \\
 q &= R_1(\tau) [q_0 \cos(\gamma - \chi) + p_0 \sin(\gamma - \chi) - u_0 (I_3 r_0 + \ell_3)^{-1} \\
 &\quad \sin \theta_0 \cos(\gamma - \chi - \varphi_0)] + u (1 + I_3 r_0 + \ell_3 - e^{-\tau})^{-1} \\
 &\quad \sin \theta_0 \cos \varphi + (I_3 - I_1)^{-1} \{ 1 + \ell_3 (I_3 - I_1) [r_0 + I_3^{-1} (1 - e^{-\tau})]^{-1} \} \ell_2, \\
 \gamma &= I_1^{-1} \{ \ell_3 \tau + (I_3 - I_1) [r_0 \tau + I_3^{-1} (\tau + e^{-\tau} - 1)] \}.
 \end{aligned}
 \tag{20}$$

It is clear from (20) that  $p$  and  $q$  behave in periodic manners, and consequently they have a stationary, stable behavior. The values of  $(\ell_1, \ell_3)$  and  $(\ell_2, \ell_3)$  have good impacts on the structures of  $p$  and  $q$  as observed in (20). Moreover, the variable  $\gamma$  is impacted by the values of

$\ell_3$ . It must be noted that all variables that depend on GM components can be used to describe the difference between the results obtained and the earlier results in [29] and [34].

### The Atmospheric Case of a Symmetric Body

In this part, we examine the following form of the restoring moment on the motion of a dynamically symmetric body

$$\begin{aligned}
 u(\tau, \theta) &= \varepsilon U(\tau, \theta) \\
 &= \varepsilon [U(\theta) + \delta \sin v\tau] = u^*(\theta) + \varepsilon \delta \sin v\tau; \\
 U(\theta) &= I_1(\mu + 2\eta \cos \theta), \quad v = \text{const.}, \quad \delta > 0, \quad \delta < 0.
 \end{aligned}
 \tag{21}$$

Here  $\eta$  and  $\mu$  denote the constant coefficients. Such works are focused on the uncontrolled 3D rotational motion of the RB in the atmospheric case [43].

Making use of (18) and (21) in (13), and then using (4) and (10) to obtain the following expressions of  $\psi, \chi, p$ , and  $q$  in the forms

$$\begin{aligned}
 \psi &= \psi_0 + U(\theta_0) \int_0^\tau (I_3 r + \ell_3)^{-1} d\tau + R_1, \\
 \chi &= \int_0^\tau [U(\theta_0) \cos \theta_0 - I_1 \eta \sin^2 \theta_0] [I_3 r + \ell_3]^{-1} d\tau + R_1 \cos \theta_0, \\
 \gamma &= I_1^{-1} \{ \ell_3 \tau + (I_3 - I_1) [r_0 \tau + I_3^{-1} (\tau + e^{-\tau} - 1)] \}, \\
 r &= I_3^{-1} \int_0^\tau k(\tau) d\tau = r_0 + I_3^{-1} (1 - e^{-\tau}); \quad k(\tau) = e^{-\tau}
 \end{aligned}$$

$$\begin{aligned}
p = & F_4 [p_0 \cos(\gamma - \chi) - q_0 \sin(\gamma - \chi) \\
& + u^*(\theta_0)(I_3 r_0 + \ell_3)^{-1} \sin \theta_0 \\
& \times \sin(\gamma - \chi - \varphi_0)] + u^*(\theta_0) \\
& [I_3 (r_0 + I_3^{-1}(1 - e^{-\tau})) + \ell_3]^{-1} \\
& \sin \theta_0 \sin \varphi + \{(I_3 - I_1)[r_0 + I_3^{-1}(1 - e^{-\tau})] + \ell_3\}^{-1} \\
& [r_0 + I_3^{-1}(1 - e^{-\tau})] \ell_1 + R_2, \quad q = F_4 [p_0 \sin(\gamma - \chi) \\
& + q_0 \cos(\gamma - \chi) - u^*(\theta_0)(I_3 r_0 + \ell_3)^{-1} \sin \theta_0 \\
& \times \cos(\gamma - \chi - \varphi_0)] + u^*(\theta_0)[I_3 (r_0 + I_3^{-1}(1 - e^{-\tau})) + \ell_3]^{-1} \\
& \sin \theta_0 \sin \varphi + \{(I_3 - I_1)[r_0 + I_3^{-1}(1 - e^{-\tau})] + \ell_3\}^{-1} \\
& [r_0 + I_3^{-1}(1 - e^{-\tau})] \ell_2 + R_3,
\end{aligned} \tag{22}$$

where

$$\begin{aligned}
R_1 = & \delta \int_0^\tau (I_3 r + \ell_3)^{-1} \sin(v\tau) d\tau, \\
R_2 = & \varepsilon \delta \sin(v\tau)(I_3 r + \ell_3)^{-1} \sin \theta_0 \sin \varphi, \\
R_3 = & \varepsilon \delta \sin(v\tau)(I_3 r + \ell_3)^{-1} \sin \theta_0 \cos \varphi, \\
F_4 = & [1 - \frac{1}{I_1(a^2 + b^2)^{1/2}} \int_0^\tau h(\tau) d\tau], \quad h(\tau) = \frac{1}{1 + \tau^2}.
\end{aligned}$$

According to (22), we can say that  $\psi$  is time-dependent in which its manner increases with the increasing of time. The projections  $p$  and  $q$  of  $\underline{\omega}$  have a periodic behavior over the entire time interval, reflecting their stability.

### Small Constant Moment Case

Here, we are going to investigate the significance of a small value of the projections  $M_j$  ( $j = 1, 2, 3$ ) of  $\underline{M}$  for the analogous rotatory body's motion of the Lagrange's case. Therefore, we examine the responses of the body to the moment of a small constant value directed along the  $Oz$  axis. To accomplish this goal, we consider that  $M_j$  have the forms [29]

$$M_1 = \varepsilon^2 M_1^* = \text{const}, \quad M_2 = \varepsilon^2 M_2^* = \text{const}, \quad M_3 = \varepsilon M_3^* = \text{const}. \tag{23}$$

Regarding the non-resonant case, the averaging system (13) takes the form

$$\begin{aligned}
a' = & -bU(I_3 r + \ell_3)^{-1} \cos \theta + \frac{b}{2} v d^2 z^{*2} s_0 \\
& \sin^2 \theta (d^2 + z^{*2} - 2dz^* \cos \theta)^{-3/2} (I_3 r + \ell_3)^{-1}, \\
b' = & aU(I_3 r + \ell_3)^{-1} \cos \theta + \frac{a}{2} v d^2 z^{*2} s_0 \\
& \sin^2 \theta (d^2 + z^{*2} - 2dz^* \cos \theta)^{-3/2} (I_3 r + \ell_3)^{-1}, \\
r' = & \varepsilon I_3^{-1} M_3^*, \quad \theta' = 0, \quad \psi' = U(I_3 r + \ell_3)^{-1}.
\end{aligned} \tag{24}$$

Integrating  $r'$  and  $\theta'$  to get

$$r = r_0 + \varepsilon I_3^{-1} M_3^* t, \quad \theta = \theta_0, \tag{25}$$

where  $r_0$  and  $\theta_0$  are integration's constants, in which  $r_0$  is an arbitrary initial value of  $r$  and  $\theta = \theta_0$  defines the constancy of the nutation angle through the motion.

Substituting (25) into the expression of  $\psi'$  in (24), the result will be

$$\psi = \psi_0 + \frac{U}{M_3^*} \ln |(I_3 r_0 + \varepsilon M_3^* t + \ell_3)|, \tag{26}$$

where  $\psi_0 = \psi_{t=0}$ .

With the aid of Eq. (25), the solution of the first two equations of (24) can be written as

$$\begin{aligned}
a = & P_0 \cos \beta + Q_0 \sin \beta - U_0(I_3 r_0 + \ell_3)^{-1} \\
& \sin \theta_0 \sin(\beta + \varphi_0), \quad b = P_0 \sin \beta - Q_0 \cos \beta \\
& + U_0(I_3 r_0 + \ell_3)^{-1} \sin \theta_0 \cos(\beta + \varphi_0); \\
\beta = & \frac{1}{M_3^*} \left[ U \cos \theta_0 + \frac{1}{2} v d^2 z^{*2} \sin^2 \theta_0 s_0 (d^2 + z^{*2} - 2dz^* \cos \theta_0)^{-3/2} \right] \\
& \ln |\varepsilon M_3^* t + I_3 r_0 + \ell_3|.
\end{aligned} \tag{27}$$

Making use of (4), (10), (25), and (27), one obtains  $p$  and  $q$  in the forms

$$\begin{aligned}
p = & p_0 \cos(\gamma - \beta) - q_0 \sin(\gamma - \beta) + u_0 (I_3 r_0 + \ell_3)^{-1} \\
& \times \sin \theta_0 \sin(\gamma - \beta - \varphi_0) + u [I_3 (r_0 + \varepsilon I_3^{-1} M_3^* t) + \ell_3]^{-1} \\
& \times \sin \theta_0 \sin \varphi_0 + \{(I_3 - I_1) + \ell_3 (r_0 + \varepsilon I_3^{-1} M_3^* t)^{-1}\}^{-1} \ell_1, \\
q = & p_0 \sin(\gamma - \beta) + q_0 \cos(\gamma - \beta) - u_0 (I_3 r_0 + \ell_3)^{-1} \\
& \times \sin \theta_0 \cos(\gamma - \beta - \varphi_0) + u [I_3 (r_0 + \varepsilon I_3^{-1} M_3^* t) + \ell_3]^{-1} \\
& \times \sin \theta_0 \cos \varphi_0 + \{(I_3 - I_1) + \ell_3 (r_0 + \varepsilon I_3^{-1} M_3^* t)^{-1}\}^{-1} \ell_2, \\
\gamma = & I_1^{-1} \left[ \ell_3 t + (I_3 - I_1) \left( r_0 t + \frac{1}{2} \varepsilon I_3^{-1} M_3^* t^2 \right) \right].
\end{aligned} \tag{28}$$

It is obvious that  $p$  and  $q$  are expressed in terms of trigonometric functions, the components  $\ell_1, \ell_3$  and  $\ell_2, \ell_3$  of the GM have a good effect on the manner of the waves illustrating  $p$  and  $q$ , respectively. Moreover, the gained results represent a generalization of those which were obtained in [29, 30], and [34] for the free motion of the GM.

### Analysis of the Results

This section is presented to discuss the achieved results of the applications in the previous section through some graphical plots. To achieve this task, the following data are considered



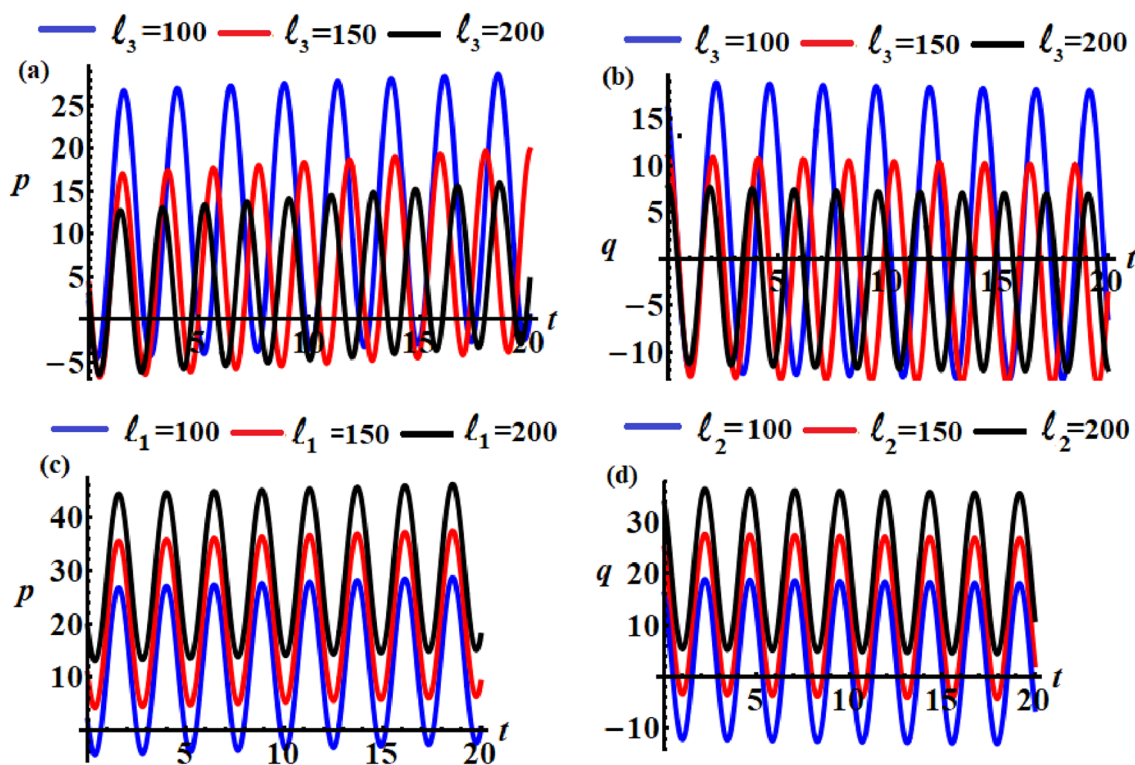


**Fig. 2** Behavior of  $p(t)$  and  $q(t)$  for the first case when **a** at  $\ell_1 = \ell_2 = 100$  and  $\ell_3 (= 100, 150, 200)$ , **b** at  $\ell_1 = \ell_2 = 100$  and  $\ell_3 (= 100, 150, 200)$ , **c** at  $\ell_2 = \ell_3 = 100$  and  $\ell_1 (= 100, 150, 200)$ , **d** at  $\ell_1 = \ell_3 = 100$  and  $\ell_2 (= 100, 150, 200)$

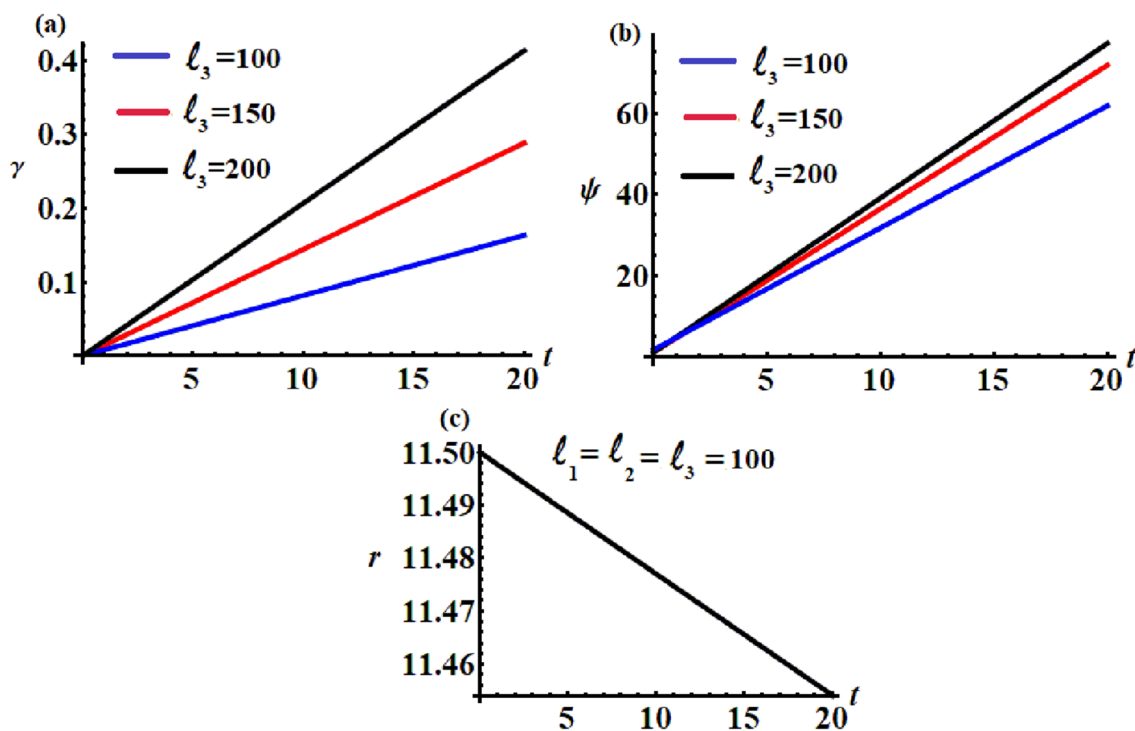


**Fig. 3** The time dependency of  $\gamma$ ,  $\psi$ , and  $r$  of the first case

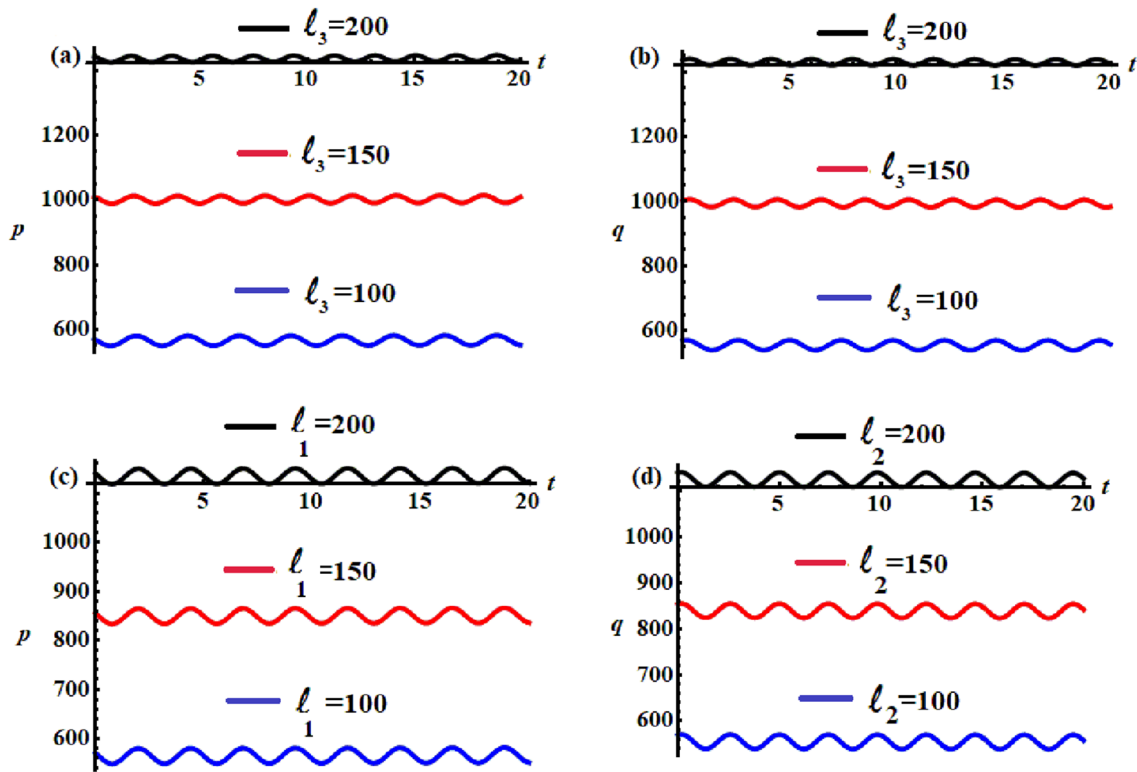


**Fig. 4** The solutions  $p(t)$  and  $q(t)$  for the second case when **a** at  $\ell_1 = \ell_2 = 100$  and  $\ell_3 (= 100, 150, 200)$ , **b** at  $\ell_1 = \ell_2 = 100$  and  $\ell_3 (= 100, 150, 200)$ , **c** at  $\ell_2 = \ell_3 = 100$  and  $\ell_1 (= 100, 150, 200)$ , **d** at  $\ell_1 = \ell_3 = 100$  and  $\ell_2 (= 100, 150, 200)$

$$\begin{aligned}
 I_1 &= 8 \text{ kg m}^2, \quad I_3 = 5 \text{ kg m}^2, \quad \varepsilon = 0.001, \\
 r_0 &= 11.5 \text{ rad s}^{-1}, \quad p_0 = 0.06 \text{ rad s}^{-1}, \quad q_0 = 0.04 \text{ rad s}^{-1}, \\
 \theta_0 &= (\pi/6) \text{ rad}, \quad \varphi_0 = (\pi/18) \text{ rad}, \quad \psi_0 = (\pi/3) \text{ rad}, \\
 m &= 200 \text{ kg}, \quad a = 1, \quad b = 1, \quad \ell_1, \ell_2, \ell_3 (= 100, 150, 200) \\
 &\text{kg m}^2 \text{ s}^{-1}, \quad g = 9.81 \text{ m s}^{-2}, \quad s_0 = 2.5, \quad \nu = 0.05, \quad h = 1.1, \\
 z^* &= 1.5, \quad L = 2.5, \quad v = 0.001, \quad \mu = 2, \quad \eta = 1, \quad \delta = 3.
 \end{aligned}$$

The principal aim of the calculations presented in Figs. 2, 3, 4, 5, 6, 7, 8 and 9 is to examine the influence of the projections  $\ell_1, \ell_2$ , and  $\ell_3$  of the GM on the body's dynamical behavior.

According to Eqs. (15) and (16) that describe the case of linear dissipative moment and based on the above data, the variations of  $p$  and  $q$  versus  $t$  are plotted graphically in Fig. 2 for different values of  $\ell_j (j = 1, 2, 3)$ . Parts (a) and (b) reveal the impact of  $\ell_3$  on these solutions. An inspection of these parts shows periodic progressive waves are obtained, in which the waves' amplitudes decrease and the oscillations number increases with the increase of  $\ell_3$  values. In contrast, the other two parts (c) and (d) of Fig. 2 explore the change of  $p$  and  $q$  when  $\ell_1$  and  $\ell_2$  have different values. It is obvious that periodic waves are graphed

where their amplitudes increase with the increase of the values of  $\ell_1$  and  $\ell_2$ .

Parts of Fig. 3 show the time behavior of angles  $\gamma$ ,  $\psi$ , and the axial angular velocity  $r$  of the first case. It is noted that the behavior of  $\gamma$  and  $\psi$  increases gradually during the examined time interval when  $\ell_3$  increases as predicted before from Eqs. (15) and (16), as shown in portions (a) and (b) while, the axial component decreases with the increase of time, as displayed in part (c).

The curves indicated in Fig. 4 reveal the changes of the solutions  $p$  and  $q$  with time  $t$  for distinct values of  $\ell_1, \ell_2$ , and  $\ell_3$  of the achieved results of the second case in Sect. 4.2. Figure 4a, b are calculated when  $\ell_3 (= 100, 150, 200) \text{ kg m}^2 \text{ s}^{-1}$ , while Fig. 4c, d are drawn when  $\ell_1$  and  $\ell_2$  have the values (100, 150, 200). In this figure, periodic waves are obtained in which they obey to the formulas of (20). It's worth noting that the components  $(\ell_1, \ell_3)$  and  $(\ell_2, \ell_3)$  have significance effect on the natural of the waves of  $p$  and  $q$ .

According to the graphs in Fig. 5, we can see that the behavior of angle  $\psi$  increases gradually with time, as seen in parts (c), (d), and (e) at the mentioned values of  $\ell_3$ . The same conclusion holds true for the behavior of  $\gamma$  and  $r$  as drawn in Fig. 5a, b, respectively.

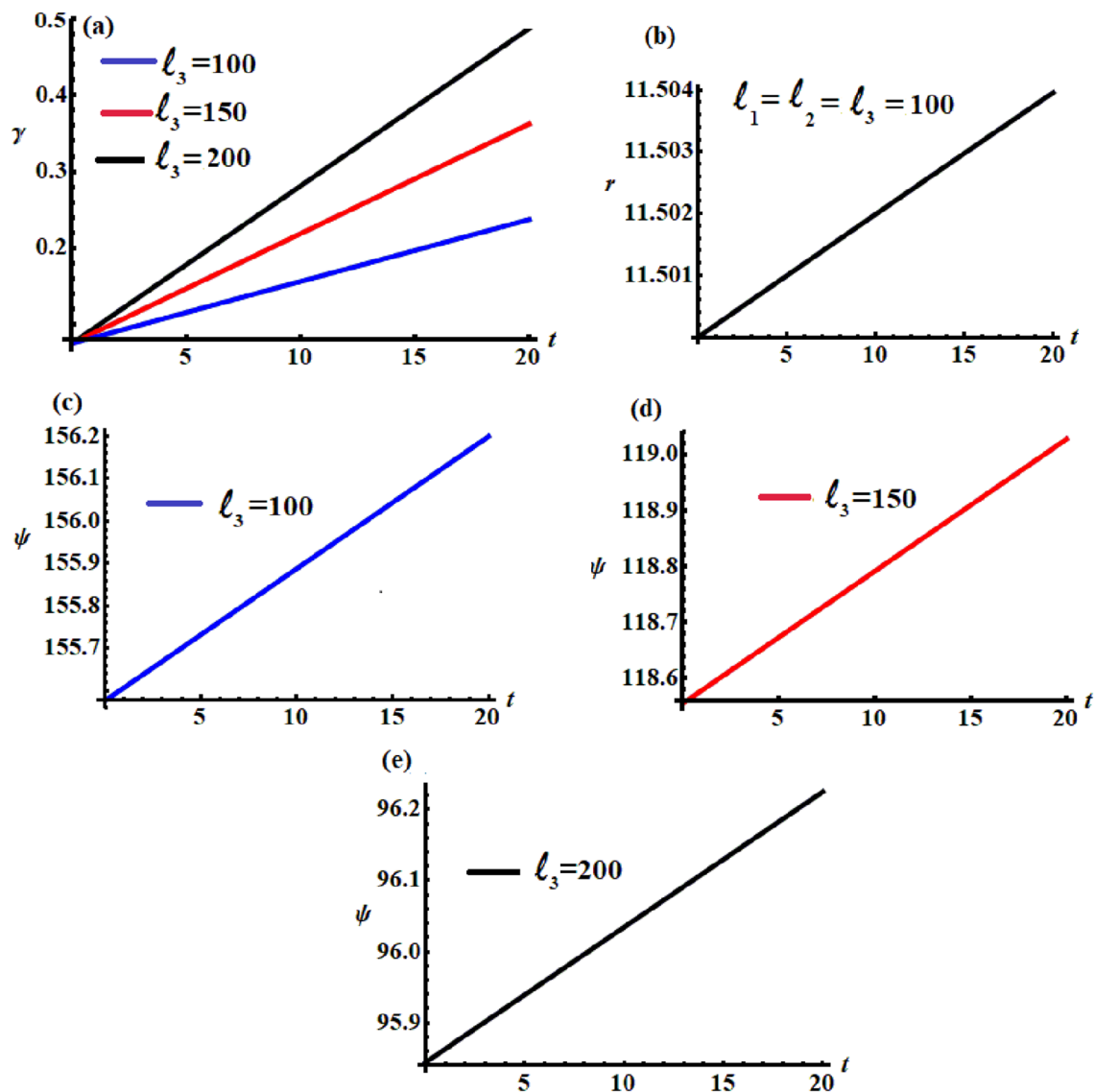


Fig. 5 The time-relations of  $\gamma$ ,  $r$ , and  $\psi$  of the second case

Parts of Fig. 6 show the change of the obtained results  $p$  and  $q$  for the atmospheric case versus time  $t$  when  $\ell_j$  ( $j = 1, 2, 3$ ) take various values. It is evident that the variation of the third projection  $\ell_3$  ( $= 100, 150, 200$ )  $\text{kg m}^2 \text{s}^{-1}$  of the GM  $\underline{\ell}$  at  $\ell_1 = \ell_2 = 100 \text{ kg m}^2 \text{s}^{-1}$  produces periodic waves, as shown in portions (a) and (b) of the considered figure, in which the waves' amplitudes increase with the increase of  $\ell_3$  values while the number of oscillations remains constant. The same concluding remarks are observed when  $\ell_1$  ( $= 100, 150, 200$ )  $\text{kg m}^2 \text{s}^{-1}$  at  $\ell_2 = \ell_3 = 100 \text{ kg m}^2 \text{s}^{-1}$  and  $\ell_2$  ( $= 100, 150, 200$ )  $\text{kg m}^2 \text{s}^{-1}$  when  $\ell_1 = \ell_3 = 100 \text{ kg m}^2 \text{s}^{-1}$  as illustrated in the other two parts (c) and (d), respectively.

The inspection of the parts of Fig. 7 reveals that the behavior of the angle  $\psi$  of precession, the self-rotation angle

$\gamma$ , and the axial angular velocity  $r$  with the time  $t$ . It is noted that the variation of the value of the component  $\ell_3$  has a positive action on the behavior of the variables  $\gamma$  and  $\psi$  as shown in parts (a) and (b). Alternatively, there is no variation of the axial angular velocity with the variation of  $\ell_3$  due to that this component does not depend on  $\ell_3$ . Based on the equations of (22), we can conclude that the behavior of the variables  $\gamma$ ,  $\psi$ , and  $r$  increases gradually, which is in line with the indicated drawing.

The objective of the portions of Fig. 8 is to discuss the time histories of the variables  $p$  and  $q$  for the fourth case according to the values of the GM projections. It is observed that the represented waves in the parts of this figure behave in periodic forms to assert the stability of the achieved outcomes. The waves' amplitudes decrease with

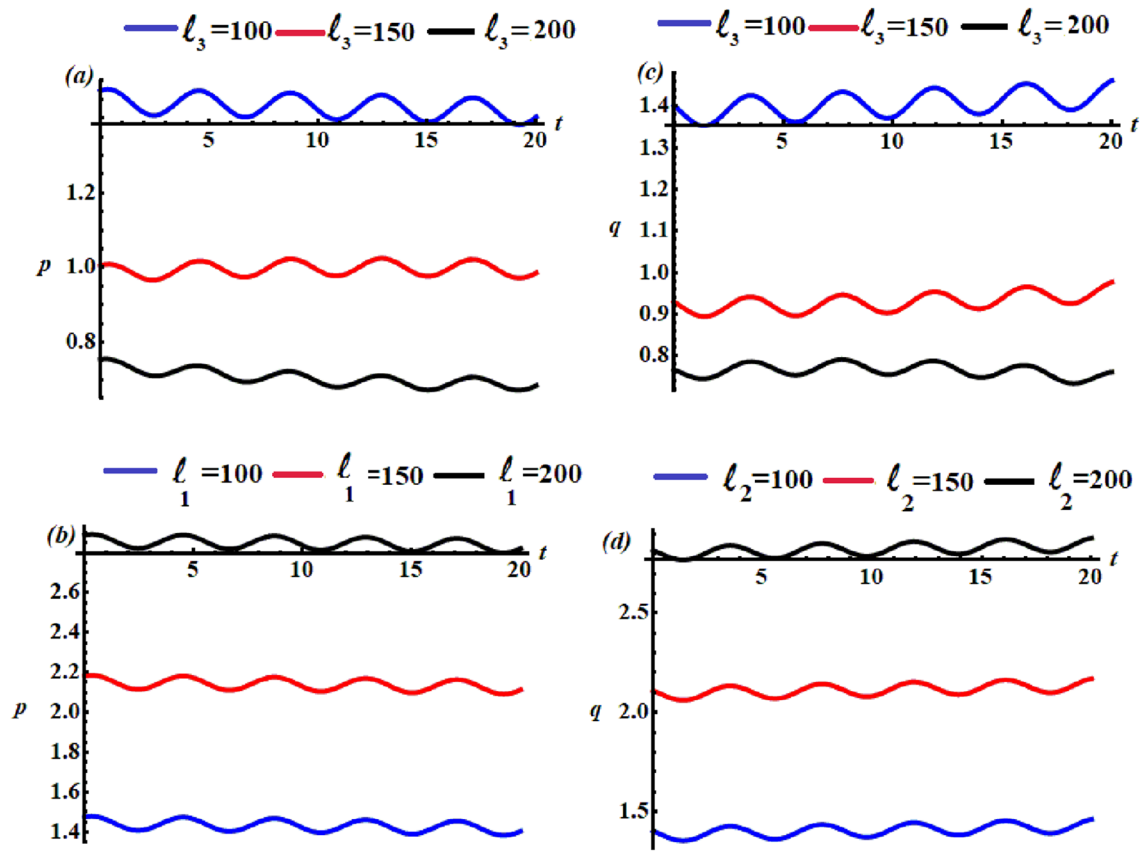


**Fig. 6** Effects of the GM on  $p$  and  $q$  for the atmospheric case of a symmetric body when **a** at  $l_1 = l_2 = 100$  and  $l_3 (= 100, 150, 200)$ , **b** at  $l_1 = l_2 = 100$  and  $l_3 (= 100, 150, 200)$ , **c** at  $l_2 = l_3 = 100$  and  $l_1 (= 100, 150, 200)$ , **d** at  $l_1 = l_3 = 100$  and  $l_2 (= 100, 150, 200)$

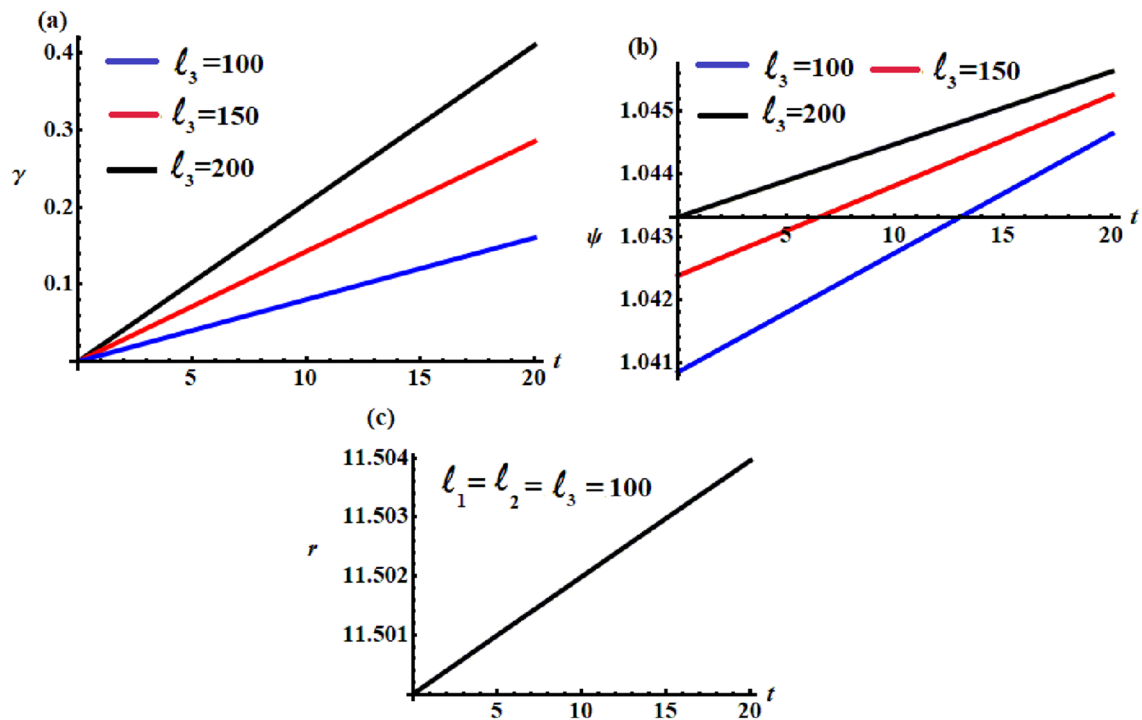


**Fig. 7** The time-dependence for  $\gamma$ ,  $\psi$ , and  $r$  of the third case

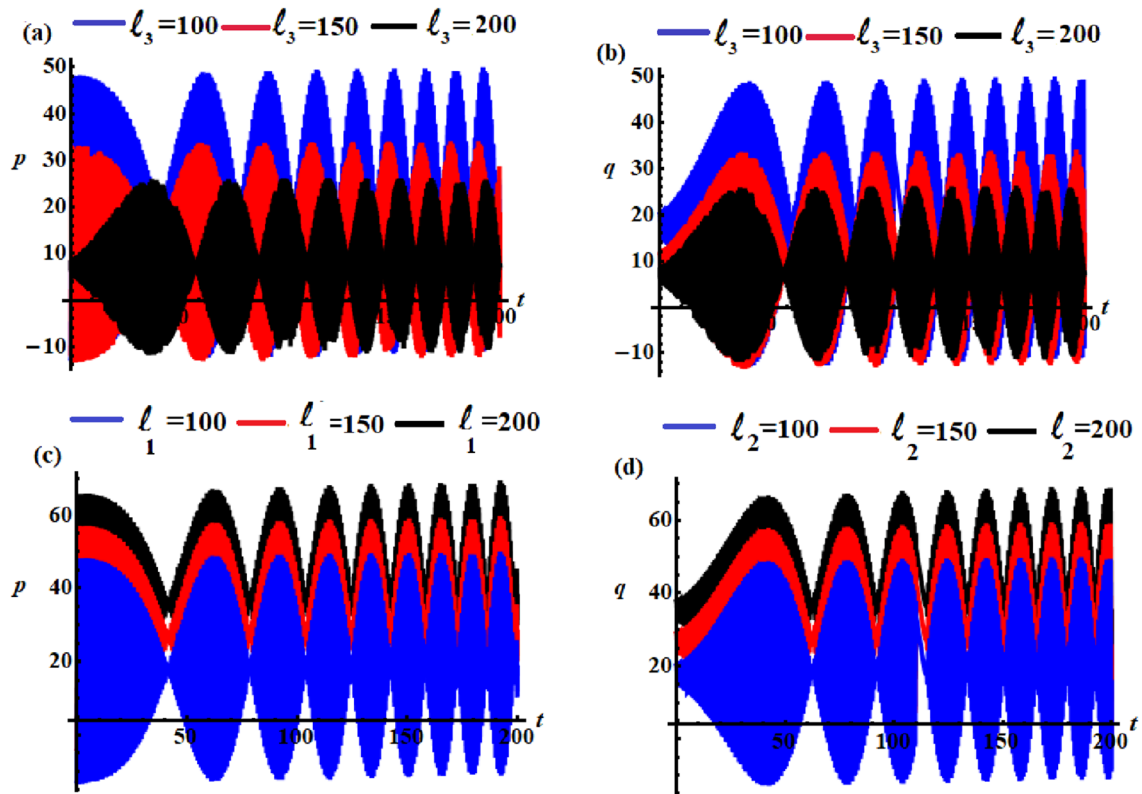


**Fig. 8** Characterizes waves of  $p$  and  $q$  with  $t$  for the fourth case when **a** at  $l_1 = l_2 = 100$  and  $l_3 (= 100, 150, 200)$ , **b** at  $l_1 = l_2 = 100$  and  $l_3 (= 100, 150, 200)$ , **c** at  $l_2 = l_3 = 100$  and  $l_1 (= 100, 150, 200)$ , **d** at  $l_1 = l_3 = 100$  and  $l_2 (= 100, 150, 200)$

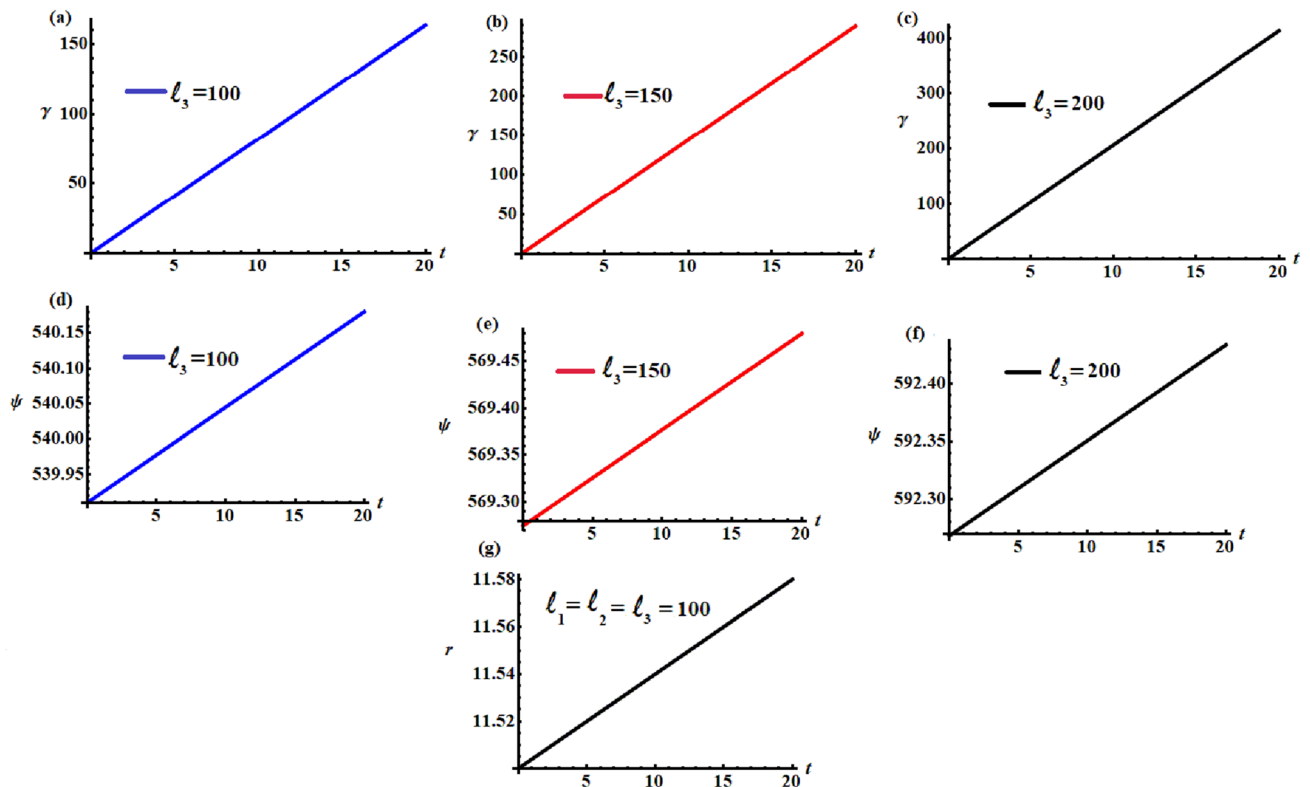


**Fig. 9** Time history of  $\gamma$ ,  $\psi$ , and  $r$  against time  $t$  of the fourth case

the increasing of  $\ell_3$  when  $\ell_1$  and  $\ell_2$  take stationary values, as shown in parts (a) and (b) of this figure, while the amplitudes of the same results increase with the increasing of  $\ell_1$  and  $\ell_2$  when  $\ell_3$  unchanged as plotted in parts (c) and (d).

Looking closely at the parts of Fig. 9, we can see that the behavior of the variables  $\gamma$ ,  $\psi$ , and  $r$  increases gradually as time goes on, in which the effect of  $\ell_3$  does not appear with the axial angular velocity  $r$  as indicated in Fig. 9g, while it appears clearly with the self-rotation angle  $\gamma$  and  $\psi$  as seen in Fig. 9a–f.

Based on the above simulation and the studied cases, we conclude that the motion of the body can be defined as having a stable behavior and being chaotic-free.

## Conclusion

The rotational motion of a symmetric RB in 3D, attached with a string, about the principal axis of dynamic symmetry has been examined. This motion is considered to be under the influence of the moments of perturbation and gyrostat, along the inertia main axes. The small parameter is inserted based on the assumptions of high angular velocity around the axis of the body's dynamic symmetry, and the projections of the perturbing moment are estimated to be less than or equal to the moment of restoring. The AM is used to yield the averaging system of the controlling EOM and to obtain the approximate analytic solutions for some important applications. The solutions of these applications have been discussed and represented graphically to explore the good effects of the considered moments on the body's dynamical behavior. Moreover, the achieved results generalize the previously related works, such as in [29, 30], and [34]. The significance of this work is due to its different engineering applications, especially in devices and vehicles that are based on vibrating systems.

**Funding** Open access funding provided by The Science, Technology & Innovation Funding Authority (STDF) in cooperation with The Egyptian Knowledge Bank (EKB). No specific grant was given to this research by any funding organisation in the public, private, or non-profit sectors.

**Data availability** Since no datasets were created or examined for this research, data sharing is not applicable.

## Declarations

**Conflict of interest** The authors affirm that they do not have any competing interests.

**Open Access** This article is licensed under a Creative Commons Attribution 4.0 International License, which permits use, sharing, adaptation, distribution and reproduction in any medium or format, as long as you give appropriate credit to the original author(s) and the source, provide a link to the Creative Commons licence, and indicate if changes were made. The images or other third party material in this article are

included in the article's Creative Commons licence, unless indicated otherwise in a credit line to the material. If material is not included in the article's Creative Commons licence and your intended use is not permitted by statutory regulation or exceeds the permitted use, you will need to obtain permission directly from the copyright holder. To view a copy of this licence, visit <http://creativecommons.org/licenses/by/4.0/>.

## References

- Nayfeh AH (2004) Perturbations methods. WILEY-VCH Verlag GmbH and Co. KGaA, Weinheim
- Bogoliubov NN, Mitropolsky YA (1961) Asymptotic methods in the theory of non-linear oscillations. Gordon and Breach, New York
- Malkin IG (1959) Some problems in the theory of nonlinear oscillations, United States Atomic Energy Commission. Technical Information Service, ABC-tr-3766
- Iu A (1963) Arkhangel'skii, On the motion about a fixed point of a fast spinning heavy solid. *J Appl Math Mech* 27:1314–1333
- El-Barki FA, Ismail AI (1995) Limiting case for the motion of a rigid body about a fixed point in the Newtonian force field. *ZAMM* 75(11):821–829
- Ismail AI, Amer TS (2002) The fast spinning motion of a rigid body in the presence of a gyrostatic momentum. *Acta Mech* 154:31–46
- Amer TS, Amer WS (2018) The rotational motion of a symmetric rigid body similar to Kovalevskaya's case. *Iran J Sci Technol Trans Sci* 42(3):1427–1438
- Amer TS (2017) On the dynamical motion of a gyro in the presence of external forces. *Adv Mech Eng* 9(2):1–13
- Amer WS (2021) Modelling and analyzing the rotatory motion of a symmetric gyrostat subjected to a Newtonian and magnetic fields. *Results Phys* 24:104102
- Ismail AI (1996) On the application of Krylov–Bogoliubov–Mitropolski technique for treating the motion about a fixed point of a fast spinning heavy solid. *ZFW* 20(4):205–208
- Amer TS, Ismail AI, Amer WS (2012) Application of the Krylov–Bogoliubov–Mitropolski technique for a rotating heavy solid under the influence of a gyrostatic moment. *J Aerospace Eng* 25(3):421–430
- Amer TS, Amer WS (2018) The substantial condition for the fourth first integral of the rigid body problem. *Math Mech Solids* 23(8):1237–1246
- Leimanis E (1965) The general problem of the motion of coupled rigid bodies about a fixed point. Springer, New York
- Yehia HM (1986) New integrable cases in the dynamics of rigid bodies. *Mech Res Commun* 13:169–172
- Yehia HM (1997) New generalizations of the integrable problems in rigid body dynamics. *J Phys A Math Gen* 30:7269–7275
- Yehia HM, Elmandouh AA (2011) New conditional integrable cases of motion of a rigid body with Kovalevskaya's configuration. *J Phys A Math Theor* 44:012001
- Elmandouh AA (2015) New integrable problems in rigid body dynamics with quartic integrals. *Acta Mech* 226:2461–2472
- Elmandouh AA (2018) New integrable problems in a rigid body dynamics with cubic integral in velocities. *Results Phys* 8:559–568
- Náprstek J, Fischer C (2016) Dynamic behavior and stability of a ball rolling inside a spherical surface under external excitation. In: Zingoni A (ed) *Insights and innovations in structural engineering, mechanics and computation*. Taylor & Francis, London, pp 214–219

20. Náprstek J, Fischer C (2020) Limit trajectories in a non-holonomic system of a ball moving inside a spherical cavity. *JVET* 8(2):269–284
21. Náprstek J, Fischer C (2021) Trajectories of a ball moving inside a spherical cavity using first integrals of the governing nonlinear system. *Nonlinear Dyn* 106:1591–1625
22. Náprstek J, Fischer C (2020) Stable and unstable solutions in auto-parametric resonance zone of a non-holonomic system. *Nonlinear Dyn* 99:299–312
23. He J-H, Amer TS, El-Kafly HF, Galal AA (2022) Modelling of the rotational motion of 6-DOF rigid body according to the Bobylev–Steklov conditions. *Results Phys* 35:105391
24. Farag AM, Amer TS, Amer WS (2022) The periodic solutions of a symmetric charged gyrostat for a slightly relocated center of mass. *Alex Eng J* 61:7155–7170
25. Amer TS, Abady IM (2017) On the application of KBM method for the 3-D motion of asymmetric rigid body. *Nonlinear Dyn* 89:1591–1609
26. Amer TS, Farag AM, Amer WS (2020) The dynamical motion of a rigid body for the case of ellipsoid inertia close to ellipsoid of rotation. *Mech Res Commun* 108:103583
27. Amer TS, El-Kafly HF, Galal AA (2021) The 3D motion of a charged solid body using the asymptotic technique of KBM. *Alex Eng J* 60:5655–5673
28. Amer WS (2017) On the motion of a flywheel in the presence of attracting center. *Results Phys* 7:1214–1220
29. Akulenko LD, Leshchenko DD, Chernousko FL (1986) Perturbed motions of a rigid body that are close to regular precession. *Izv Akad Nauk SSSR MTT* 21(5):3–10
30. Leshchenko DD, Sallam SN (1990) Perturbed rotation of a rigid body relative to fixed point. *Mech Solids* 25(5):16–23
31. Akulenko L, Leshchenko D, Kushpil T, Timoshenko I (2001) Problems of evolution of a rigid body under the action of perturbing moments. *Multibody Syst Dyn* 6(1):3–16
32. Leshchenko D, Ershkov S, Kozachenko T (2022) Rotations of a rigid body close to the Lagrange case under the action of nonstationary perturbation torque. *J Appl Comput Mech* 8(3):1023–1031
33. Leshchenko D, Ershkov S, Kozachenko T (2022) Evolution of motion of a rigid body similar to Lagrange top under the influence of slowly time varying torques. *Proc IMechE Part C J Mech Eng Sci* 236(22):10879–10890
34. Akulenko LD, Leshchenko DD, Kozachenko TA (2002) Evolution of rotations of a rigid body under the action of restoring and control moments. *J Comput Syst Sci* 41(5):868–874
35. Amer TS (2008) On the rotational motion of a gyrostat about a fixed point with mass distribution. *Nonlinear Dyn* 54:189–198
36. Amer TS (2016) The rotational motion of the electromagnetic symmetric rigid body. *Appl Math Inf Sci* 10(4):1453–1464
37. Ismail AI, Amer TS, El Banna SA (2012) Electromagnetic gyroscopic motion. *J Appl Math* 2012:1–14
38. Amer TS, Abady IM (2018) On the motion of a gyro in the presence of a Newtonian force field and applied moments. *Math Mech Solids* 23(9):1263–1273
39. Galal AA, Amer TS, El-Kafly H, Amer WS (2020) The asymptotic solutions of the governing system of a charged symmetric body under the influence of external torques. *Results Phys* 18:103160
40. Amer WS (2019) The dynamical motion of a gyroscope subjected to applied moments. *Results Phys* 12:1429–1435
41. Chernousko FL, Akulenko LD, Leshchenko DD (2017) *Evolution of motions of a rigid body about its center of mass*. Springer, Cham
42. Akulenko LD (1987) *Asymptotic methods in optimal control*. Nauka, Moscow
43. Aslanov VS, Serov VM (1995) Rotation of an axisymmetric rigid body with biharmonic characteristic of the restoring torque. *Mech Solids* 30(3):15–20

**Publisher's Note** Springer Nature remains neutral with regard to jurisdictional claims in published maps and institutional affiliations.